IBRO Neuroscience Reports 18 (2025) 528–538

Contents lists available at ScienceDirect

IBRO Neuroscience Reports

journal homepage: www.sciencedirect.com/journal/IBRO-Neuroscience-Reports

Neuroprotective effects and mechanisms of the YiQiWenYangSanHan formula on Parkinson's disease mice

Jinling Liu [a,b,1], Dong Di [a,b,1], Suping Sun [a,b], Yan Sun [a,b], Shihan Zhou [a,b], Jing Liu [a,b], Zizhen Qin [a,b], Xinyu Yang [a,b], Xiao Wang [a,b], Zheng Xu [a,b,*], Boran Zhu [a,b,*], Haoxin Wu [a,b,*]

[a] Nanjing University of Chinese Medicine, Nanjing, Jiangsu 210023, China
[b] Key Laboratory of Integrative Biomedicine for Brain Diseases, College of Traditional Chinese Medicine, Nanjing University of Chinese Medicine, Nanjing, Jiangsu 210046, China

ARTICLE INFO

Keywords:
Parkinson's disease
YiQiWenYangSanHan formula
Neuroinflammation
Mitochondrial dysfunction
α-synuclein

ABSTRACT

Background: Parkinson's disease (PD) is a complex neurodegenerative disease, which is often treated with obvious side effects such as dopamine replacement therapy. Our team has validated the unique advantages of the traditional Chinese medicine formula, YiQiWenYangSanHan formula (YQWYSHF), through in vitro experiments, confirming its therapeutic potential for PD. Nevertheless, further research and validation are required to fully understand its protective effects and underlying mechanisms against PD.

Aim of this review: This study employed an in vivo model to investigate the effects of YQWYSHF on motor impairments, neuroinflammation, and mitochondrial dysfunction in C57BL/6 J mice caused by MPTP.

Materials and methods: Sixty C57BL/6 J mice were randomly divided into 5 groups, all groups except the control group were intraperitoneally administered MPTP for 7 days (30 mg/kg). After 4 weeks of drug intragastric treatment, we assessed the dyskinesia of mice treated with different doses of YQWYSHF by behavioral examination. Additionally, immunofluorescence was used to examine the expression of ionized calcium binding adaptor protein 1 (IBA1) and glial fibrillary acidic protein-positive (GFAP) cells. Western blotting was used to assess the expression level of tyrosine hydroxylase (TH), pyrin domain-containing 3 protein (NLRP3), apoptosis-associated speck-like proteins (ASC), cysteine-containing aspartate protease-1 (Caspase-1), interleukin-1β (IL-1β), α-synuclein (α-syn), poly (ADP-ribose) polymerase 1 (PARP1), and poly ADP ribose (PAR). Furthermore, transmission electron microscopy revealed mitochondrial impairment in the neuronal cells of the substantia nigra (SN).

Results: YQWYSHF treatment alleviated dyskinesia in a mouse model of PD. Moreover, it increased the TH expression, and could reverse the increase of IBA1, GFAP, NLRP3, ASC, caspase-1,IL-1β, α-syn, PARP1 and PAR proteins induced by MPTP.

Conclusions: YQWYSHF protects dopaminergic neurons in PD by attenuating neuroinflammation and mitochondrial dysfunction. This study provides new evidence for the clinical application of traditional Chinese medicine in the treatment of PD.

1. Introduction

Parkinson's disease (PD) stands as a common neurodegenerative condition, trailing behind Alzheimer's disease. The primary clinical manifestations include resting tremor, bradykinesia, rigidity, and non-motor symptoms, such as cognitive deficits, depression, and autonomic dysfunction (Xie and Hu, 2022). Characteristic histopathological features of PD include the depletion of dopaminergic neurons in the midbrain's nigral areas and unusual clustering of α-syn in the Lewy vesicles (Chen and Geng, 2023). The prevalence of PD increases with

* Correspondence to: Key Laboratory of Integrative Biomedicine for Brain Diseases, College of Traditional Chinese Medicine, Nanjing University of Chinese Medicine, Nanjing, Jiangsu, China.
E-mail addresses: Xuzheng@njucm.edu.cn (Z. Xu), Zhuboran@njucm.edu.cn (B. Zhu), haoxinwu@njucm.edu.cn (H. Wu).
[1] Jinling Liu and Dong Di contributed equally to this work.

https://doi.org/10.1016/j.ibneur.2025.03.014
Received 10 November 2024; Received in revised form 30 March 2025; Accepted 31 March 2025
Available online 1 April 2025

age, reaching its most significant levels in the population aged 65 and above, with a particularly sharp rise observed in those exceeding 80 years of age (Ou et al., 2021). Currently, only levodopa replacement therapy and surgical treatment can partially reduce the symptoms. However, treatment is always accompanied by several side effects, such as the 'switch phenomenon' and the 'end-of-dose phenomenon', and these treatments cannot reverse or delay the natural pathological process of the disease (Tambasco et al., 2018).

TCM compounds, extracts and prescriptions has unique advantages in improving quality of life by alleviating motor and non-motor symptoms with fewer side effects (Chang et al., 2020). Chen et al., discussed the therapeutic mechanisms against PD from the perspective of TCM itself (Chen et al., 2022a). Wu et al., summarized the protective mechanisms of paeonol on the central nervous system, discovering that paeonol can improve neuroinflammation, oxidative stress, and neuronal apoptosis in both in vitro and in vivo models of PD, and inhibit the proliferation of astrocytes in the substantia nigra (Wu et al., 2024). Chen et al., summarized ginsenoside Rd as natural neuroprotective agent that play an important role in alleviating nerve damage associated with neurodegenerative diseases such as PD (Chen et al., 2022b).

YQWYSHF, also known as Yishen Chuchan decoction (YCD) (Di et al., 2024), is a PD treatment method based on clinical experience, which is composed of *Astragalus mongholicus* Bunge, *Rehmannia glutinosa* (Gaertn.) DC., *Aconitum carmichaelii* Debeaux, *Aconitum kusnezoffii* Rchb., *Cistanche deserticola* Y.C.Ma and *Gardenia jasminoides* J. Ellis, as shown in Table S1. It has been demonstrated that the active components of YQWYSHF yield beneficial therapeutic outcomes in animal models of PD (Zhang et al., 2021a; Yang et al., 2019; Wang et al., 2019a). Our team has previously performed network pharmacological analyses and verified the therapeutic mechanism of YQWYSHF in vitro (Di et al., 2024). A total of 65 active compounds were collected from YQWYSHF, as shown in Table S2. Network pharmacology analysis has revealed multiple potential connections between YQWYSHF and PD, including biological processes, cellular components, and molecular functions, which may exert their effects through various signaling pathways. In vitro experiments have shown that the serum from rats medicated with YQWYSHF can significantly enhance the viability of SH-SY5Y cell lines treated with rotenone and reduce cell apoptosis. Furthermore, we have found that YQWYSHF can increase the expression of microtubule-associated protein 2 (MAP2). In the YQWYSHF-medicated serum, the level of superoxide dismutase (SOD) increased, while the level of reactive oxygen species (ROS) decreased, and the levels of interleukin-6 (IL-6), interleukin-1 beta (IL-1β), and tumor necrosis factor-alpha (TNF-α) were also reduced, indicating that YQWYSHF can effectively suppress cellular oxidative stress and inflammation. It is worth mentioning that the YQWYSHF-medicated serum can also significantly reduce the overexpression of p-p38 protein induced by rotenone.

Inflammation of the central nervous system (CNS) is a natural immune reaction under pathological conditions, excessive inflammatory responses can damage neurons and accelerate neurodegenerative pathologies (Kölliker-Frers et al., 2021). leading to the deterioration of dopaminergic neurons in the brain, thereby intensifying the pathological advancement of PD (Hinkle et al., 2022). Microglia and astrocytes are the primary glial cell types involved in neuroinflammation (Kölliker-Frers et al., 2021). Inflammasomes are macromolecular protein complexes present in various brain cells, including microglia and astrocytes; among these, NLRP3 inflammasome stands as the initial identified and extensively researched inflammasome, bearing the closest relation to PD, encompassing the sensor NLRP3, apoptosis-associated speck-like proteins (ASC), and the effector cysteine-containing aspartate protease-1 (caspase-1) (Zhang et al., 2021b). NLRP3 triggers the creation of the inflammasome through its interaction with ASC and activating pro-caspase-1 to produce active caspase-1. This process subsequently transforms the cytokine precursors, pro-IL-1β and pro-IL-18, into mature IL-1β and IL-18, respectively (Wang et al., 2020). Meanwhile, the aggregated α-synuclein (α-syn) is taken up by microglia, which can act as an internal warning signal to trigger NLRP3 inflammasomes and activate caspase-1, leading to the development and release of IL-1β, thereby exacerbating harm to dopaminergic neurons (Pike et al., 2021).

Mitochondrial dysfunction also leads to activation of the NLRP3 inflammasome (Xian et al., 2022). Both mitochondrial reactive oxygen species (ROS) activation and mitochondrial DNA release are believed to be critical factors mediating NLRP3 inflammasome activation (Qiu et al., 2022; Mills et al., 2017). Mitochondria-associated programmed cell death involves the overactivation of poly (ADP-ribose) polymerase 1 (PARP1), which relies on the mitochondria-associated inducible factor (AIF) nuclear translocation death pathway (Weiß et al., 2023). Mitochondrial function and α-syn also interact, and the accumulated pathological α-syn can preferentially bind to mitochondria and inhibit mitochondrial protein input, resulting in impaired mitochondrial function and impaired cellular respiration (Wang et al., 2019b). Pathological α-syn, through activation of nitric oxide synthase, activates PARP1 when DNA is mild to severely damaged, resulting in substantial production of poly ADP ribose (PAR) polymers and subsequent cell death through the Parthanatos pathway (Tang et al., 2019). Subsequently, PAR production accelerates the formation of pathological α-syn. Kam et al (Kam et al., 2018). termed this a 'feed-forward loop'.

In this study, we investigated whether YQWYSHF has a potential therapeutic effect on neurons during MPTP-induced PD and explored whether this prescription can provide a reliable experimental basis for relieving neuroinflammation and mitochondrial damage in PD, providing further evidence for the clinical value of traditional Chinese medicine.

2. Methods

2.1. Drug preparation

Every medicine in YQWYSHF is purchased from the National Medical Hall of Nanjing University of Traditional Chinese Medicine, Medicinal Material Department (Nanjing, China), where the herb quality was assessed. It was certified by Professor Haoxin Wu (School of Traditional Chinese Medicine, Nanjing University of Chinese Medicine, and School of Integrative Medicine). Voucher specimens of *Astragalus mongholicus* Bunge (voucher number: NZY-ZHU-2022001), *Rehmannia glutinosa* (Gaertn.) DC. (voucher number: NZY-ZHU-2022002), *Cistanche deserticola* Y.C.Ma (voucher number: NZY-ZHU-2022003), *Gardenia jasminoides* J.Ellis (voucher number: NZY-ZHU-2022004), *Aconitum carmichaelii* Debeaux (voucher number: NZY-ZHU-2022005) and *Aconitum kusnezoffii* Rchb. (voucher number: NZY-ZHU-2022006) had been deposited in the Herbarium of Key Laboratory of Integrative Biomedicine for Brain Diseases, Nanjing University of Chinese medicine.

The fundamental principle of traditional Chinese herbal decoction preparation involves extracting bioactive components from medicinal herbs through water-based heating and boiling processes. This method facilitates the extraction of active constituents into an aqueous solution, enhancing their bioavailability for human absorption. Moreover, the thermal process promotes potential chemical interactions among the herbal components, which may lead to synergistic therapeutic effects while potentially reducing adverse reactions. Our decoction preparation protocol is rigorously developed based on well-established traditional methods, ensuring its reliability and scientific validity. Initially, *Aconitum carmichaelii* Debeaux and *Aconitum kusnezoffii* Rchb. (20 ± 1 g each) were immersed in 0.32 L of purified water for 30 minutes, followed by rapid boiling using high heat and subsequent 40 minutes simmering at reduced heat. This prolonged heating process is crucial for reducing the toxicity of aconitine alkaloids. Subsequently, a mixture of purified water (0.84 L), Astragalus m*ongholicus* Bunge (60 ± 2 g), *Rehmannia glutinosa* (Gaertn.) DC. (20 ± 1 g), *Cistanche deserticola* Y.C. Ma (15 ± 1 g), and *Gardenia jasminoides* J.Ellis (10 ± 1 g), which had

been similarly simmered for 45 minutes, was added to the decoction vessel containing the previously prepared Aconitum species. This combined mixture was then subjected to an additional 30 minutes boiling process. The resulting decoction was filtered through a double-layer sterile gauze to obtain the primary filtrate. The residual herbal material underwent a second extraction with 0.8 L of purified water through a 30 minutes boiling process. Both filtrates were combined and concentrated to a final volume of 273.33 mL using a rotary evaporator under controlled temperature conditions. The concentrated decoction was aliquoted and stored at −20℃ in sterile containers for subsequent experimental use. To assess the quality of various YQWYSHF batches, a Waters 2695 Alliance HPLC system (Waters Corporation, Milford, MA, USA) was employed. The high-pressure liquid chromatography profile is shown in Figure S1. Madopar (100 mg/kg) (Shanghai Roche Pharmaceutical Co., Ltd., batch number YT0200) was used in parallel during the treatments.

2.2. Experimental animals

C57BL/6 J mice (6 ± 2 weeks old, 18 ± 5 g, male) were purchased from Shanghai SLAC Laboratory Animal Co., Ltd. All animal experiments adhered to the Laboratory Animal Use and Care Principles and received approval from Nanjing University of Traditional Chinese Medicine's Institutional Animal Care and Use Committee to reduce animal distress (Approval number: 202206A049). Every mouse was housed in an environment devoid of specific pathogens. The temperature of the environment is 20–24℃, the humidity is 40~60 %, and the day and night are alternating for 12 hours. The animals were provided ad libitum access to food and beverages. Each cage contained four mice.

2.3. Experimental design

Following one week of adaptive feeding mice, all groups except the control group were intraperitoneally administered MPTP for 7 days (30 mg/kg) (Tan et al., 2020). Simultaneously with modeling PD, the control group received 7 days of intraperitoneal injection with the same administered volume of saline and 4 weeks of saline gavage; the MPTP group received 7 days of intraperitoneal injection of MPTP and 4 weeks of saline gavage. The dosage of human and experimental mice was equivalent to converted (Xu et al., 2002).The YQWYSHF (18.85 g/kg) group was administered YQWYSHF by gavage at 18.85 g/kg for 4 weeks. The YQWYSHF (37.7 g/kg) group was administered YQWYSHF by gavage at 37.7 g/kg for 4 weeks. The madopar group was administered 100 mg/kg (Zhang et al., 2017; Wu et al., 2022) of madopar by gavage for 4 weeks. The MPTP was weighed, dissolved in saline at 30 mg/kg, and used immediately. The body weight and locomotor changes were observed in each mouse during the study period. Behavioral tests and sampling were performed after 4 weeks. After a 4-week feeding period, mice received anesthesia using 1 % sodium pentobarbital (intraperitoneally, 30 mg/kg). Right after being extracted, the brain tissues underwent dissection and were cleansed using a solution of phosphate-buffered saline (PBS). Furthermore, the SN in brain tissues underwent dissection in liquid nitrogen and were preserved at −80°C for additional analysis. Fig. 1.

2.4. Pole test

We assessed the locomotor ability of the mice using a pole-climbing test. Before modeling, we trained the mice to turn their heads from the pole's apex (measuring 50 cm tall and 1 cm wide) and climb smoothly to the bottom. At the beginning of the formal test, the cumulative duration required for the mice to rotate their heads and descend to the base was calculated.

2.5. Rotarod test

Acclimatization training was performed before testing. Parameter settings were as follows: The initial speed was set to 5 rpm and was accelerated to 10 rpm during the training period. On the test day, three experiments were conducted at a speed of 10 rpm. The time when the mice dropped the rotor bar was automatically recorded as the drop latency, and the average of three experiments was calculated.

2.6. Immunofluorescence staining

After heart perfusion, brain tissue was extracted and stored in 4 % paraformaldehyde at 4℃ for 48 h. The brain tissue was dissected and frozen for 48 hours with 30 % sucrose. Coronal sections of frozen brain tissue were prepared after embedding. The frozen sections were taken out and restored to RT, soaked in 4 % paraformaldehyde solution for 15 min, cleaned with PBS 3 times for 5 min each time, the brain tissue was enclosed, and the sections were immersed in 0.3 % Triton X-100 PBS and incubated at RT for 30 min. Sections of the SN portion of the brain were incubated with anti-glial fibrillary acidic protein (GFAP) antibody (GB15100–100, Servicebio, 1:500) and anti-ionized calcium-binding adaptor protein 1 (IBA1) antibody (GB15105–100, Servicebio, 1:300) to monitor glial cell growth, and with anti-tyrosine hydroxylase (TH) antibody (GB15181–100, Servicebio, 1:800) to assess dopaminergic neuron harm, and incubated in a wet box at 4℃ overnight. On the second day, the primary antibody was washed with PBS 3 times for 5 min each time, the secondary antibody was added with drops, the secondary antibody was incubated at RT without light for 2 h, the secondary antibody was washed and dried at RT, and the substania nigra of the rat brain was observed under a fluorescence microscope. The film was taken and stored, and the fluorescence intensity was analyzed using Image J.

2.7. Transmission electron microscopy

Fresh mouse SN was dissected, and the measured tissue volume was maintained at 1 × 1 × 1 mm, and it was swiftly preserved by electron microscope fixative (G1102, Servicebio) at 4°C for 3 h. The sample was washed with PBS 3 times for 5 min each time. Subsequently, stabilization was achieved with a mixture of 1 % osmium acid and PBS at RT for 2 h. Following this, the sample was washed with PBS 3 times for 5 min each time. Subsequently, the tissue underwent a cleansing process with

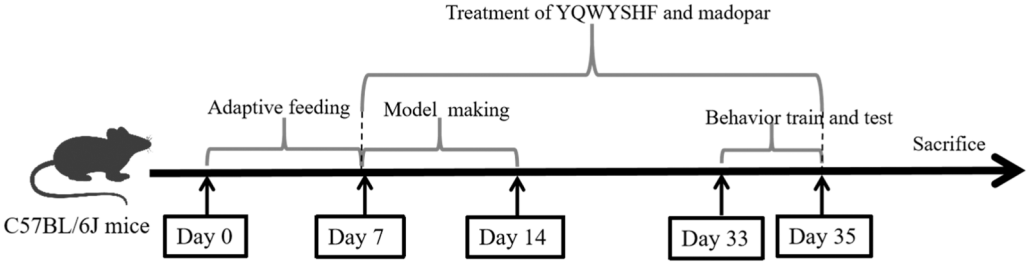

Fig. 1. Experimental design for the MPTP-induced Parkinson's disease mice.

a solution of 0.1 M phosphate buffer, and graded tandem ethanol was used for dehydration. After embedding the dehydrated tissues in an 812 embedding agent (SPI, 90529–77–4) for 5 h, the specimens were incubated in an embedding plate and oven at 37°C throughout the night, followed by slicing into 60 ultrathin segments using an ultrathin slicer. Sections underwent a dual staining process using uranium-lead (comprising 2 % uranyl acetate saturated alcohol and lead citrate, each for 15 min). They were subsequently allowed to air dry at RT throughout the night. The sections were observed using a transmission electron microscope, followed by the gathering of images for examination.

2.8. Western blotting

For the last six mice in each group, the SN extracted from their brain tissue was blended in RIPA lysis buffer and spun at 12,000 rpm for 15 min in a centrifuge having a 13.5 cm radius. NANODROP 2000 (Thermo Fisher Scientific) was used to measure the protein levels. Protein lysates were heated to a temperature of 100°C for 5 min and preserved at −70℃. The protein extracts were then moved onto PVDF membranes for additional examination. The membranes underwent blocking using 5 % skimmed milk for 1 h at RT, succeeded by an overnight incubation at 4℃ with these primary antibodies: TH (#58844, 1:1000), NLRP3 (#15101, 1:1000), Caspase-1 (#24232, 1:1000), ASC (#67824, 1:1000), IL-1β (#12426, 1:1000), α-syn (#51510, 1:1000), PAR (#83732, 1:1000), PARP (#9542, 1:1000) were obtained from Cell Signaling Technology. GAPDH (60004–1-lg, 1:10000), and β-actin (66009–1-Ig, 1:2000) were purchased from Proteintech. The next day, a supplementary goat anti-rabbit IgG H+L antibody (ZB-2306, ZSGB-BIO, 1:2000) was introduced and left to incubate with the membrane at ambient temperature for 2 h. Subsequently, the secondary antibody was cleansed, and after adding ECL luminescent solution dropwise, the strip was placed in the developer for development, the band density was assessed via ImageJ analysis software, and the proportion of the gray-scale values of the target proteins to the internal reference proteins, β-actin and GAPDH, were determined. The analysis of all outcomes was performed using GraphPad Prism 9.0 (GraphPad software).

3. Results

3.1. YQWYSHF ameliorated MPTP-induced behavioral deficits and body weight changes in mice

We first investigated whether YQWYSHF could facilitate the recovery of behavioral deficits in a mouse model of PD. PD symptoms were triggered in mice through the injection of MPTP, as previously described. Mice in the MPTP group showed a dull and lifeless coat, depression, reduced activity, muscle twitching, and tail rigidity.

We compared the changes in body weight at the start of modeling and drug treatment with MPTP over 4 weeks in the formal trial (Fig. 2A). Except for mice in the control group, which gained normal body weight, mice in the other groups lost body weight during the modeling period. From the sixth day onwards, the weight of mice in the YQWYSHF (37.7 g/kg) and madopar groups began to increase, and over time, mice

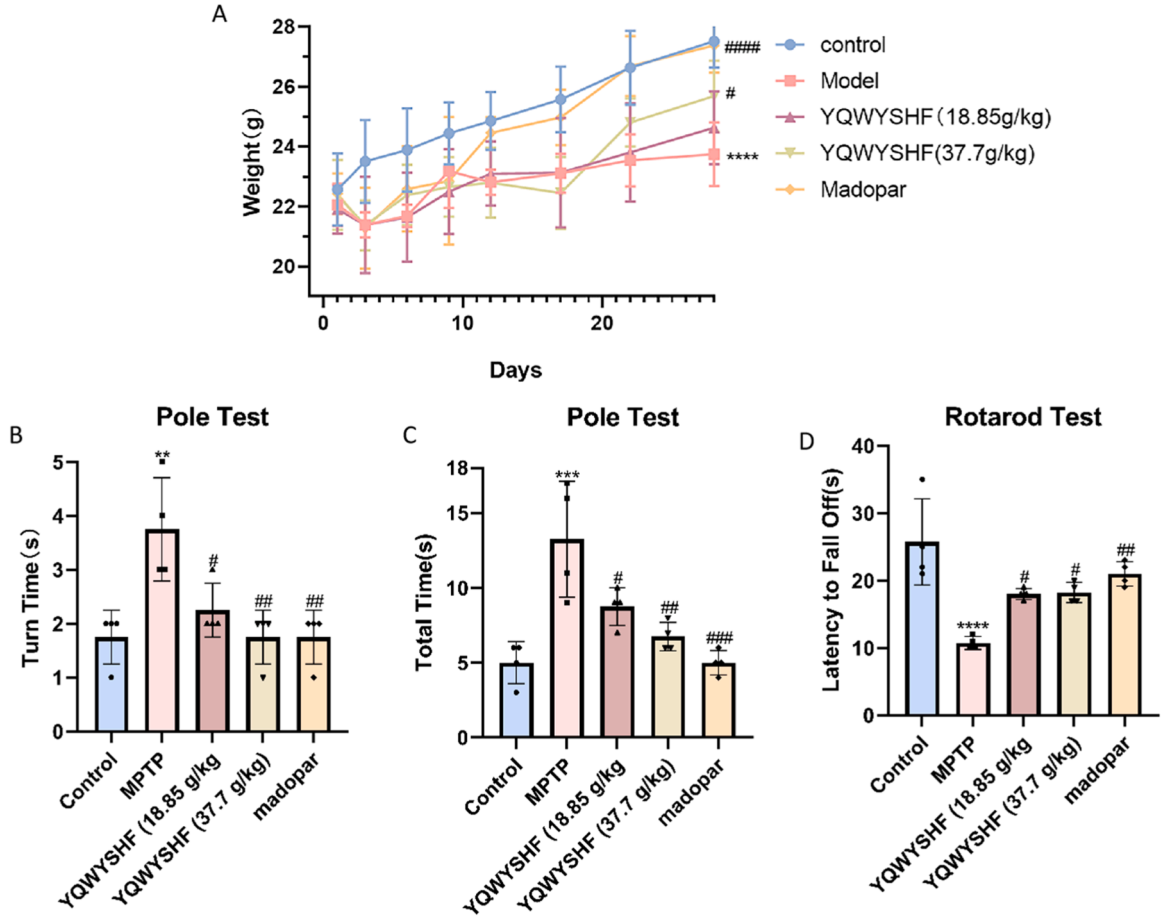

Fig. 2. Changes in body weight and motor function of mice during modeling and treatment administration. (A) Trends in body weight changes in mice during modeling administration (n = 7). (B, C) Turn time and total time devoted to the pole test (n = 4). (D) The time spent on the pole in the rotating pole test (n = 4). The data is displayed as an average ± Standard Error of the Mean. *$p < 0.05$, * *$p < 0.01$, * **$p < 0.001$, and * ** *$p < 0.0001$ in comparison to the control group; #$p < 0.05$, ##$p < 0.01$, and ###$p < 0.0001$ when compared to the MPTP group.

in the madopar group regained their position compared to those in the control group ($P < 0.0001$). The YQWYSHF (18.85 g/kg) and YQWYSHF (37.7 g/kg) groups ($P < 0.05$) gradually approached the control group, suggesting that madopar and YQWYSHF could alleviate MPTP-induced weight loss in mice.

Additionally, the effect of these medications on motor abilities in PD mice was examined. As can be seen from the results of behavioral tests (Fig. 2B-D), in the pole test, compared with the control group, the MPTP group had a significant increase in the retention time at the top turn and the total time on the pole ($P < 0.01$, $P < 0.001$). After drug treatment, YQWYSHF (18.85 g/kg) group ($P < 0.05$, $P < 0.05$), YQWYSHF (37.7 g/kg) ($P < 0.01$, $P < 0.01$) and madopar group ($P < 0.01$, $P < 0.001$) tended to shorten the time of MPTP group. Compared with the control group, the time spent on the rotarod test in MPTP group was significantly reduced ($P < 0.0001$), indicating that the motor coordination ability of mice was significantly decreased after modeling. The time spent on the device in YQWYSHF (18.85 g/kg) group ($P < 0.05$), YQWYSHF (37.7 g/kg) group ($P < 0.05$), and madopar group ($P < 0.01$) was significantly increased. The results showed that the motor balance ability and physical strength of mice were restored after drug treatment. Moreover, the cut-off limit of the turn time of the pole climbing is 2.5 s, the cut-off limit of the total time is 7.5 s, and the cut-off limit of the rotarod test is 16.5 s. In the pole test, YQWYSHF (37.7 g /kg) groups are generally smaller than the cut-off limit. In the rotarod test, the cut-off limit was higher in all treatment groups. Therefore, YQWYSHF can improve the behavioral disorders observed in MPTP-induced mice.

3.2. *YQWYSHF reduces the dopaminergic neurotoxicity caused by MPTP in mice*

Immunofluorescence staining was employed to monitor the depletion of dopaminergic neurons in the SN area in both the MPTP and drug-administered groups. Western blotting was employed to evaluate TH protein levels in each group. Immunofluorescence staining revealed a severe loss of TH-positive neuronal fibers in the SN of MPTP-induced mice (Fig. 3A). In contrast, both the YQWYSHF and madopar groups

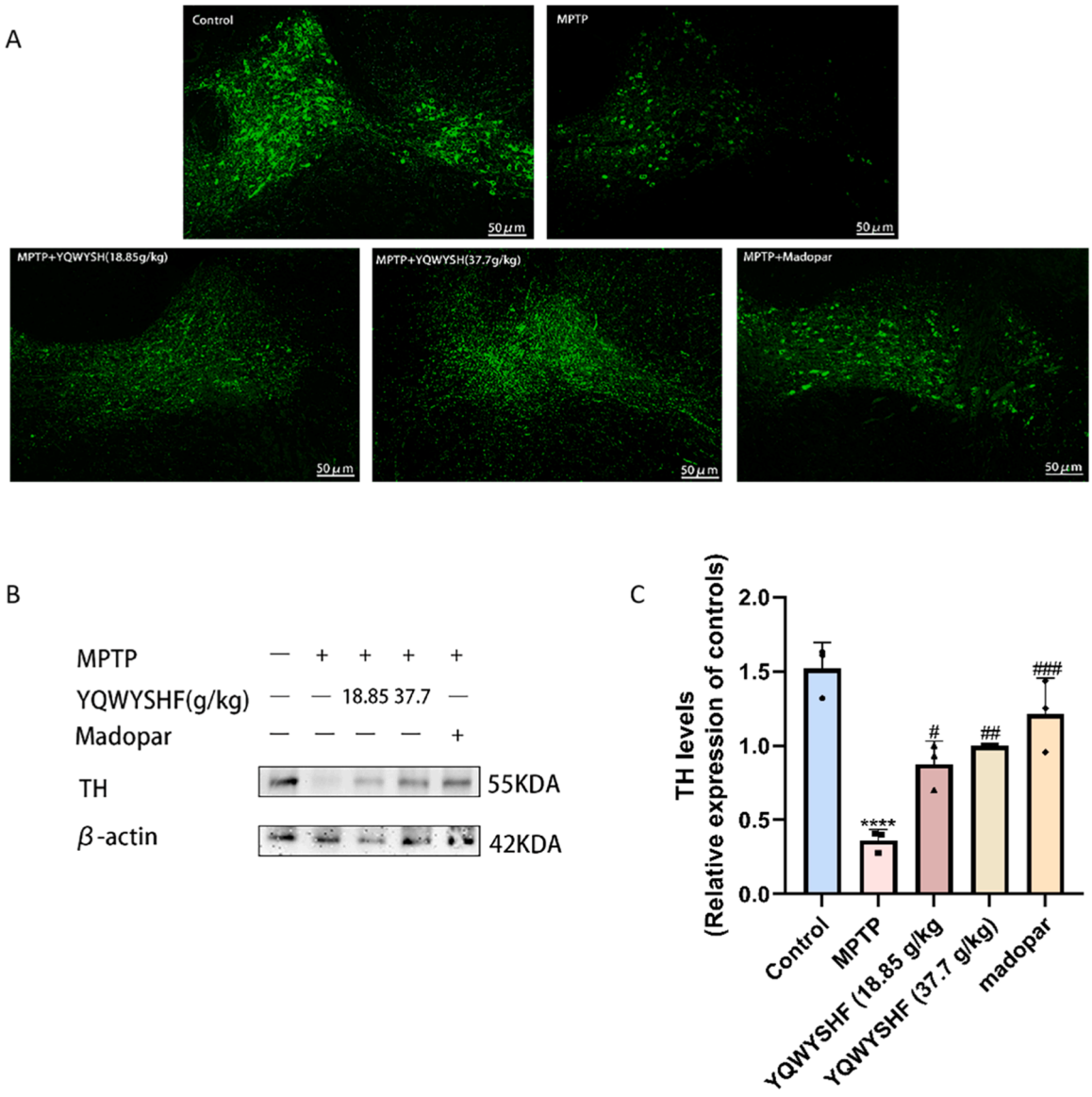

Fig. 3. Dopaminergic protective effect of YQWYSHF in a MPTP-induced PD model. (A) Typical immunofluorescence coloration for tyrosine hydroxylase (TH) across various SN groups. (B) Representative Western blot images of TH levels in the SN. The complete blots are shown in Supplementary Fig. 2. (C) Statistical analysis of TH levels in the SN (n = 3). The data is displayed as an average ± Standard Error of the Mean. *$p < 0.05$, * *$p < 0.01$, * **$p < 0.001$, and * ** *$p < 0.0001$ in comparison to the control group; #$p < 0.05$, ##$p < 0.01$, and ###$p < 0.0001$ when compared to the MPTP group.

showed significant effects on TH recovery. Western Blot showed that TH protein expression in MPTP group decreased significantly compared with control group ($P < 0.001$). The TH protein level of SN in YQWYSHF (18.85 g/kg) group ($P < 0.05$), YQWYSHF (37.7 g/kg) group ($P < 0.05$) and madopar group ($P < 0.01$) was significantly higher than MPTP group (Fig. 3B, C). Therefore, YQWYSHF can reduce damage to dopaminergic neurons in PD.

3.3. YQWYSHF inhibits MPTP-induced microglia and astrocyte proliferation

Microglia and astrocytes are well known to proliferate in MPTP-induced mice; therefore, we evaluated whether YQWYSHF could reduce the proliferation of these cells following MPTP treatment. We performed double immunofluorescence staining for the microglia marker, IBA1, and the astrocyte marker, GFAP (Fig. 4A-D). The positive area of microglia ($P < 0.01$) and astrocytes ($P < 0.01$) in MPTP group was significantly higher than control group. YQWYSHF (18.85 g/kg) group, YQWYSHF (37.7 g/kg) group and madopar group alleviated the proliferation of MPTP-induced glia-positive area ($P < 0.01$). Consequently, YQWYSHF mitigates dopamine-induced harm in PD mice through the decreased growth of microglia and astrocytes.

3.4. YQWYSHF mitigates the neuroinflammation linked to NLRP3 in mice induced by MPTP

NLRP3 expression in the SN of mouse brain tissues across groups was detected using Western blotting to investigate the effect of YQWYSHF on NLRP3 inflammasomes in a living organism (Fig. 5A-E). NLRP3 ($P < 0.01$), Caspase-1 ($P < 0.001$), ASC ($P < 0.001$), and IL-1β ($P < 0.0001$) levels were significantly increased in MPTP group compared with control group. The expression of ASC ($P < 0.05$) and IL-1β ($P < 0.05$) in YQWYSHF (18.85 g/kg) group was decreased. YQWYSHF (37.7 g/kg) group and madopar group had significant decrease on NLRP3 ($P < 0.05$, $P < 0.05$), Caspase-1 ($P < 0.05$, $P < 0.01$), ASC ($P < 0.01$, $P < 0.01$) and IL-1β ($P < 0.01$, $P < 0.01$) proteins in SN region, which hindered NLRP3 inflammasomes activation, indicating YQWYSHF potential to lessen neuronal harm in PD through NLRP3 inflammasome inhibition.

3.5. YQWYSHF ameliorates mitochondrial damage in vivo

Following the assessment of the effect of YQWYSHF on NLRP3 inflammasomes in vivo, our investigation focused on whether YQWYSHF ameliorated MPTP-induced and parthanatos-related mitochondrial damage in mice. Western blotting was used to analyze the

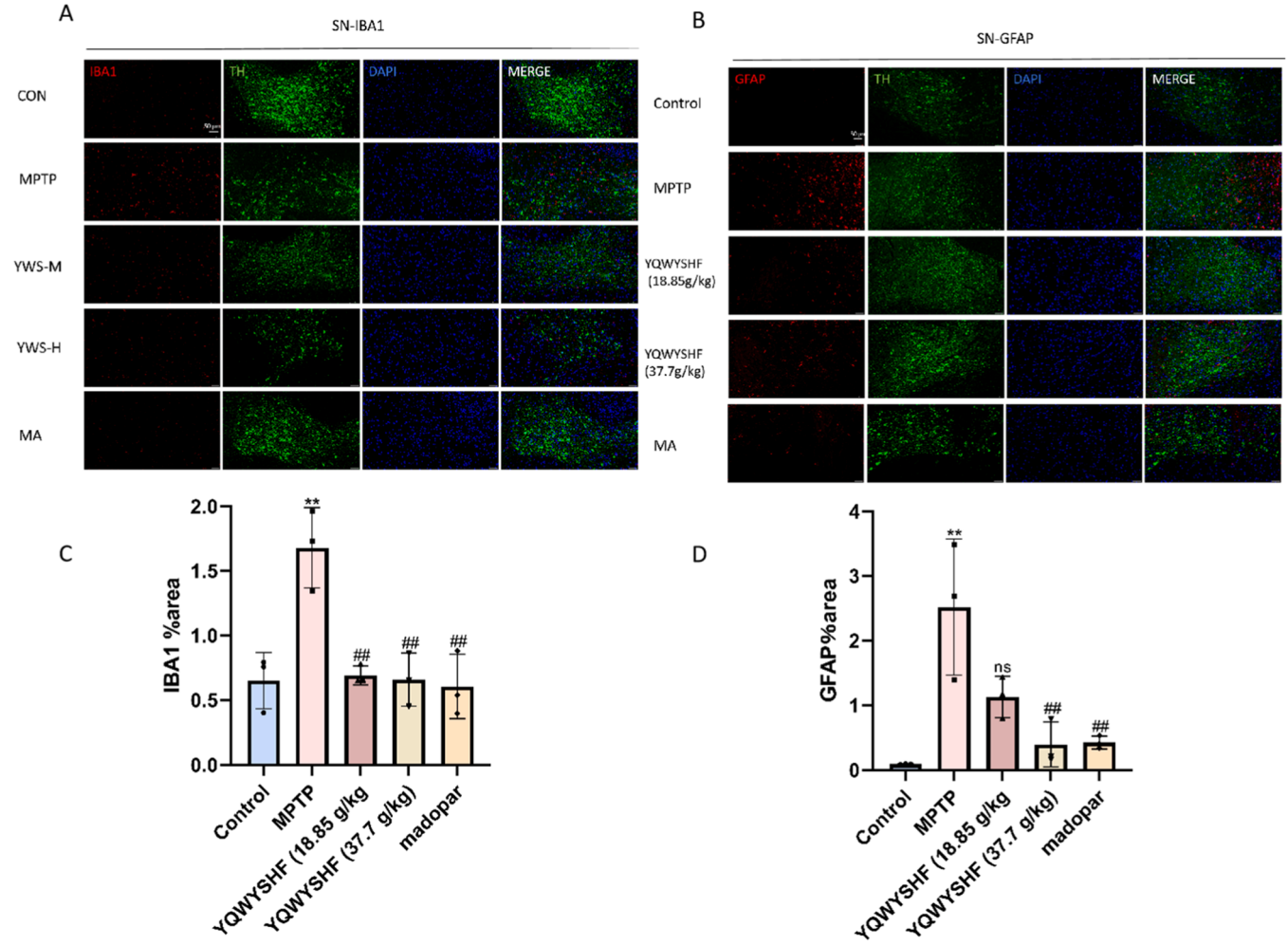

Fig. 4. YQWYSHF acts as an inhibitor to the MPTP-triggered growth of microglia and astrocytes. (A, C) Immunofluorescence staining of microglia in the SN that are IBA1-positive (red), TH (green), and DAPI (blue) shows that YQWYSHF significantly reduces MPTP-induced activation of microglia (n = 3). (B, D) Immunofluorescence staining of astrocytes in the SN positive for GFAP (red), TH (green), and DAPI (blue) shows that YQWYSHF significantly reduces MPTP-induced astrocyte activation (n = 3). The data is displayed as an average ± Standard Error of the Mean. *$p < 0.05$, * *$p < 0.01$, * **$p < 0.001$, and * ** *$p < 0.0001$ in comparison to the control group; #$p < 0.05$, ##$p < 0.01$, and ###$p < 0.0001$ when compared to the MPTP group.

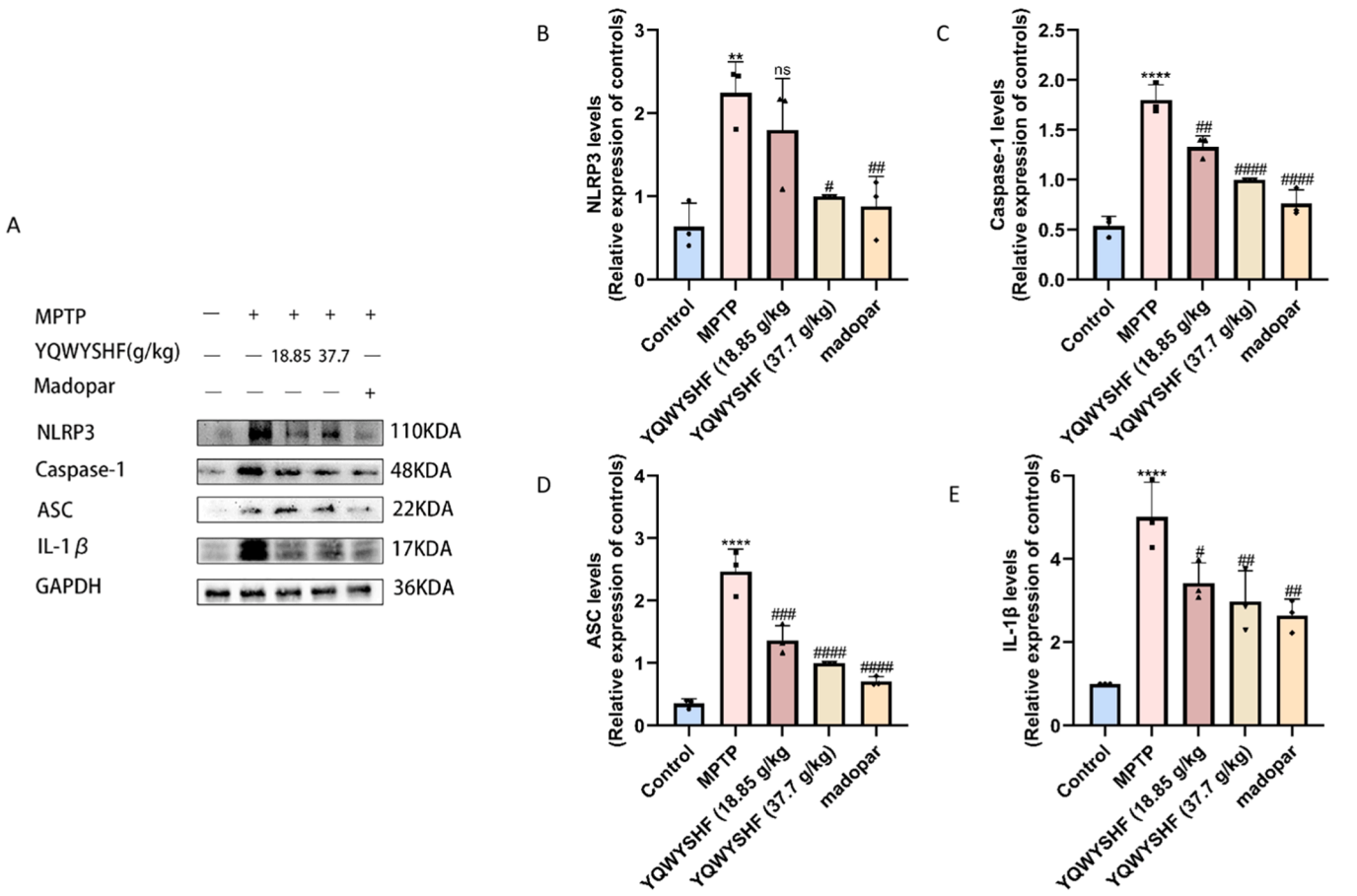

Fig. 5. YQWYSHF mitigates the neuroinflammation linked to NLRP3 in the SN. (A) Exemplary Western blot bands and graphs depict the statistical evaluation of NLRP3, Caspase-1, ASC, and IL-1β expression levels in the SN. The complete blots are shown in Supplementary Fig. 3. (B-E) The ratios of densitometry values for NLRP3, Caspase-1, ASC, and IL-1β to GAPDH in the SN were calculated and normalized to each respective control culture (n = 3). The data is displayed as an average ± Standard Error of the Mean. *$p < 0.05$, * *$p < 0.01$, * **$p < 0.001$, and * ** *$p < 0.0001$ in comparison to the control group; #$p < 0.05$, ##$p < 0.01$, and ###$p < 0.0001$ when compared to the MPTP group.

concentrations of α-syn, PARP1, and PAR proteins in the SN area of the mice's brains in each group. In the SN, compared with control group, MPTP group increased the expression of PARP1 ($P < 0.01$), PAR ($P < 0.001$), and α-syn ($P < 0.001$) proteins in SN region, while drug treatment reduces the expression of these proteins. The downregulation effects of PARP1 ($P < 0.05$, $P < 0.01$), PAR ($P < 0.01$, $P < 0.01$), and α-syn ($P < 0.05$, $P < 0.01$) in YQWYSHF (37.7 g/kg) and madopar groups were significantly different from those in MPTP group. (Fig. 6A-D). YQWYSHF inhibited PARP1 activation and aggregation in vivo, thereby ameliorating mitochondrial damage.

The state of mitochondria within neuronal cells in the SN was monitored using transmission electron microscopy, and the results revealed that the mitochondria in the control group were structurally normal, with intact membranes, homogeneous matrix, and parallel arrangement of cristae (Fig. 6E). The mitochondria in the MPTP and YQWYSHF (18.85 g/kg) groups were obviously swollen, with the intra-membranous matrix dissolved, cristae not visible, and vacuolated-like degeneration. The mitochondria in the YQWYSHF (37.7 g/kg) group were mildly swollen, the intra-membraneous matrix was locally faded, and the cristae were broken and reduced. Most mitochondria in the madopar group were mildly swollen with intact membranes, localized matrix dilution, and broken cristae. Overall, it appears that high-dose YQWYSHF partially restored the mitochondrial status of cells in the PD model.

4. Discussion

Contemporary pharmacological research has demonstrated that specific bioactive components within YQWYSHF exhibit significant dopaminergic neuroprotective properties, suggesting therapeutic potential for neurodegenerative disorders. These neuroprotective compounds, as systematically documented in Supplementary Table 2 of our supplementary materials, have been identified through comprehensive literature review (Xiao et al., 2022; Gao et al., 2018, 2020; Zhang et al., 2021c). PD, a critical neurodegenerative condition, is pathologically marked by motor function impairment due to the deterioration of dopaminergic neurons in the SN. An increasing number of research indicates that neuroinflammation and mitochondrial malfunction play significant roles as altering elements in PD (Pizarro-Galleguillos et al., 2023). Currently, effective drugs for patients with PD are lacking (Liu et al., 2020). Therefore, this study evaluated the therapeutic effects of YQWYSHF in experimental PD and investigated whether the mechanism of its neuroprotective effect was related to neuroinflammation and mitochondrial dysfunction.

The correct choice of modeling method according to the experimental needs is an important part of conducting studies on the efficacy and mechanism of drugs for PD. MPTP traverses the blood-brain barrier, initially broken down by monoamine oxidase B into 1-methyl-4-phenyl-2,3-dihydropyridine (MPDP+), before transforming into harmful 1-methyl-4-phenylpyridinium ions (MPP+). MPP+ enters the dopaminergic neurons, suppresses mitochondrial respiratory chain complex I, diminishes ATP levels, and increases ROS production, which can mimic

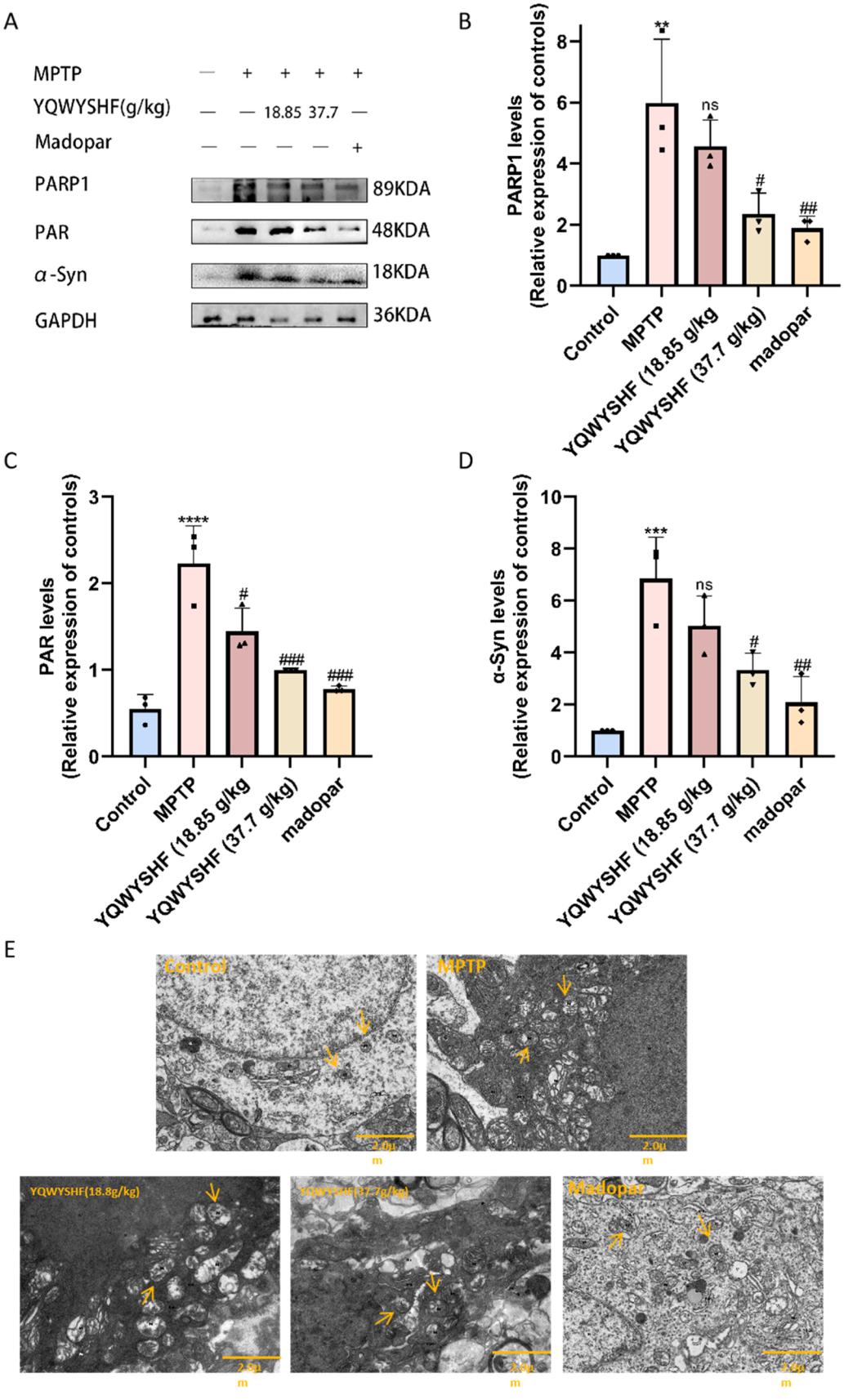

(caption on next page)

Fig. 6. YQWYSHF protects the neurons by reducing mitochondrial dysfunction. (A) The concentrations of α-syn, PARP1, and PAR proteins in the SN were identified using Western blot analysis. The complete blots are shown in Supplementary Fig. 4. (B-D) The ratios of densitometry values for α-syn, PARP1, and PAR to GAPDH in the SN were calculated and normalized to each respective control culture (n = 3). (E) The state of mitochondria within neuronal cells in the SN was monitored using transmission electron microscopy. All data are presented as means ± Standard Error of the Mean (n = 3). Exemplary electron microscopic images of the SN for each category. Yellow arrow: Mitochondria. The data is displayed as an average ± Standard Error of the Mean. *$p < 0.05$, * *$p < 0.01$, * **$p < 0.001$, and * ** *$p < 0.0001$ in comparison to the control group; #$p < 0.05$, ##$p < 0.01$, and ###$p < 0.0001$ when compared to the MPTP group.

various biochemical features of PD pathogenesis (Zhu et al., 2022). The subacute MPTP mouse model has previously demonstrated severe dopaminergic neuron loss and marked astrocyte proliferation (Zhang et al., 2017); therefore, the model selected in the present study is commonly used in PD research. It can nearly replicate the pathological and biochemical changes in PD and has the advantages of a short modeling time and a clear genetic background. In this experiment, the mice showed symptoms similar to PD, such as decreased body mass, tail rigidity, slow movement, and tremor, indicating that the modeling was successful. The pole and rotarod test is a commonly used experiment to evaluate the motor state of PD mouse models, and it is used to evaluate the motor coordination and balance ability of mice. In our behavioral tests, YQWYSHF can partially improve motor disorders in PD mice, with pole climbing outcomes indicating a prolonged time for MPTP-stimulated mice to reverse and ascend from the highest to the lowest point compared to the control group. In the rotarod test, mice in the MPTP group also dropped faster, which may be due to the reduced movement of the mice after modeling; the movement showed static tremors, resulting in reduced motor capacity. However, the motor ability of mice improved after treatment with different doses of YQWYSHF, suggesting that YQWYSHF can ameliorate motor disorders in mice.

Tyrosine is the initial synthetic substrate for human synthesis of DA, the most critical of which is TH. The activity of this enzyme determines the content of DA in nerve cells, and the level of its content in the brain can directly reflect the condition of PD (Jayanti et al., 2022). In the results of immunofluorescence and Western Blot experiments, we can see that the content of TH in the brain of mice decreased under the intervention of MPTP, and recovered under the intervention of YQWYSHF, which alleviated the damage of DA neurons to a certain extent.

Microglia are one of the major glial cell types involved in the inflammatory response in the CNS. The M1 phenotype of activated microglia amplifies local inflammation by releasing multiple inflammatory mediators and cytotoxic factors (Guo et al., 2022). In addition, astrocytes can transform into the toxic A1 phenotype due to pro-inflammatory factors released by activated microglia, which drives synaptic degeneration and induces necrosis in dopaminergic neurons through the secretion of neurotoxins or the release of multiple complement components. These cells can induce a vicious cycle of neuroinflammation when acting simultaneously, thereby exacerbating the inflammatory response (Giovannoni and Quintana, 2020). A wide variety of inflammasomes exist, of which the NLRP3 inflammasome is the most popular one currently under study and is widely present in microglia and other immune cells in the brain, it is composed of NLRP3, ASC and Caspase-1 (Zhang et al., 2023). When the NLRP3 inflammasome senses α-syn aggregates or microglia secrete IL-1β, the junctional protein ASC is triggered, recruiting and activating caspase-1. This triggers the secretion of pro-inflammatory cytokines, IL-1β, and IL-18, amplifying the inflammatory response in the PD cell model and exacerbating the degeneration and necrosis of dopaminergic neurons and α-syn aggregates (Calabresi et al., 2023). Our experimental results showed that compared with the control group, nigra microglia and astrocytes in MPTP group were activated, NLRP3 inflammatory-related protein expression was enhanced, IL-1β, secretion was increased. After YQWYSHF and madopar intervention,IBA1 and GFAP expression was decreased in the SN of PD mice, NLRP3 inflammatory-associated protein decreased, and IL-1β, secretion is reduced. Therefore, we concluded that YQWYSHF reduced neuronal damage in PD by suppressing glial cell activation and regulation of the NLRP3.

Mitochondria are the energy supply stations of cells and the basis of various cellular activities. Dysfunction in mitochondria is a key contributor to the deterioration of dopaminergic neurons and a key element in the development of PD (Yao et al., 2024). Mitochondrial dysfunction is intrinsically linked to α-syn aggregation, and recent studies have demonstrated (Giamogante et al., 2024) that soluble α-syn impacts both lysosomal and mitochondrial operations, along with autophagy processes. Hyperaggregation of α-syn is also a key regulator of NLRP3 during neuroinflammation, which modulates NLRP3 through the TLR receptor pathways, mitochondrial pathway, and autophagy, exacerbating neuroinflammation progression and dopaminergic neuronal damage (Huang et al., 2023). Parthanatos occurs widely in neurodegenerative disorders. A critical pathway is the signaling of PAR polymers to mitochondria, which mediate the translocation of AIF from the mitochondria to the nucleus. Previous studies (Kam et al., 2018) have demonstrated that α-syn in early PD patients' brains causes an increase in PARP-1 activity, producing more PAR polymers, and these PAR polymers further exacerbate α-syn accumulation. We detected the relevant indicators of mitochondrial function in the SN of each group of mice through Western blotting. Then we observed the recovery of mitochondrial damage in the SN of the mice after YQWYSHF treatment by transmission electron microscopy. The results showed that MPTP upregulated factors associated with mitochondrial dysfunction, including α-syn, PARP1, and PAR. After YQWYSHF treatment, these proportions were significantly downregulated. Transmission electron microscopy revealed that YQWYSHF (37.7 g/kg) also partially restored mitochondrial morphology, including damage to the matrix and ridge. This implies that the healing effect of YQWYSHF could be governed by a relentless loop of α-syn-PARP1-PAR, which regulates mitochondrial function.

Our research has some limitations. On one hand, this study only examined the nigrostriatal region to investigate the mechanism of cognitive impairment. In contrast, the striatum, hippocampus, and other brain regions are related to amateur cognitive function. The molecular biology of other brain regions can be potentially investigated in the future. Additionally, although this experimental model of PD is safe, simple, and operable, it may not adequately reflect the natural course of PD, which exhibits a multi-system chronic progression.

5. Conclusion

YQWYSHF has a preventive effect in a PD mouse model, significantly improving motor dysfunction and reducing neuroinflammatory responses by suppressing of the NLRP3 inflammasome. It also reduces mitochondrial dysfunction and protects dopaminergic neurons. This provides strong evidence for the efficacy of traditional Chinese medicinal practices in managing PD.

Abbreviations

PD Parkinson's Disease
YQWYSHF YiQiWenYangSanHan formula
TH Tyrosine hydroxylase
ASC Apoptosis-associated speck-like protein containing
ATPAdenosine Triphosphate
NLRP3 pyrin domain-containing 3 protein

Caspase-1Cysteine-containing aspartate protease-1
IL-1βInterleukin-1β
α-synα-synuclein
PARPoly (ADP-ribose)
PARP1Poly (ADP-ribose) polymerase-1
MPTP1-methyl-4-phenyl-1,2,3,6-tetrahydropyridine
SNSubstantia Nigra
IBA-1Ionized calcium binding adaptor protein 1
GFAPGlial fibrillary acidic protein

CRediT authorship contribution statement

Zhu Boran: Writing – review & editing, Project administration, Methodology, Funding acquisition, Conceptualization. **Xu Zheng:** Writing – original draft, Supervision, Methodology, Funding acquisition, Conceptualization. **Wang Xiao:** Software, Resources. **Yang Xinyu:** Software, Resources. **Qin Zizhen:** Data curation. **Liu Jing:** Software, Formal analysis. **Zhou Shihan:** Validation, Software. **Sun Yan:** Visualization, Investigation. **Sun Suping:** Visualization, Investigation. **Liu Jinling:** Writing – original draft, Methodology, Investigation, Formal analysis. **Di Dong:** Writing – original draft, Methodology, Investigation. **Wu Haoxin:** Writing – review & editing.

Conflict of interests and compliance with ethical standards statement

The authors declare that they have no competing financial interests or personal relationships that may have influenced the work reported in this study.

Declaration of Competing Interest

The authors declare that they have no known competing financial interests or personal relationships that could have appeared to influence the work reported in this paper.

Acknowledgments

This research project was supported by the National Science Foundation of China (82074292), Natural Science Foundation of Jiangsu Province of China (BK20230447), Jiangsu Traditional Chinese Medicine Science and Technology Development Project (QN202202), Luo LinXiu Teacher Development Fund Project (LLX202312), NATCM's Project of High-level Construction of Key TCM Disciplines (GSPZDXK-FJXZD002, GSPZDXK-FJXYB018), and Nanjing University of Traditional Chinese Medicine College Student Innovation Training Program Plan (202310315111Y).

Appendix A. Supporting information

Supplementary data associated with this article can be found in the online version at doi:10.1016/j.ibneur.2025.03.014.

Data availability

The raw data supporting the conclusions of this manuscript will be available from the corresponding author upon reasonable request.

References

Xie, L.L., Hu, L.D., 2022. Research progress in the early diagnosis of Parkinson's disease. Neurol. Sci. 43 (11), 6225–6231.
Chen, P., Geng, X., 2023. Research progress on the kynurenine pathway in the prevention and treatment of Parkinson's disease. J. Enzym. Inhib. Med. Chem. 38 (1), 2225800.
Ou, Z., Pan, J., Tang, S., et al., 2021. Global trends in the incidence, prevalence, and years lived with disability of Parkinson's disease in 204 countries/territories From 1990 to 2019. Front. Public Health 9, 776847.
Tambasco, N., Romoli, M., Calabresi, P., 2018. Levodopa in Parkinson's disease: current status and future developments. Curr. Neuropharmacol. 16, 1239–1252.
Chang, Y.M., Manoj Kumar, M., Lu, C.Y., et al., 2020. Parkinson's disease a futile entangle of Mankind's credence on an herbal remedy: a review. Life Sci. 257, 118019.
Chen, P., Zhang, J., Wang, C., et al., 2022a. The pathogenesis and treatment mechanism of Parkinson's disease from the perspective of traditional Chinese medicine. Phytomedicine 100, 154044.
Wu, R., Liu, Y., Zhang, F., et al., 2024. Protective mechanism of Paeonol on central nervous system. Phytother. Res 38 (2), 470–488.
Chen, Y.Y., Liu, Q.P., An, P., et al., 2022b. Ginsenoside Rd: a promising natural neuroprotective agent. Phytomedicine 95, 153883.
Di, D., Zhang, C., Sun, S., et al., 2024. Mechanism of Yishen Chuchan decoction intervention of Parkinson's disease based on network pharmacology and experimental verification. Heliyon 10 (14), e34823.
Zhang, X., Liu, K., Shi, M., et al., 2021a. Therapeutic potential of catalpol and geniposide in Alzheimer's and Parkinson's diseases: a snapshot of their underlying mechanisms. Brain Res Bull. 174, 281–295.
Yang, C., Mo, Y., Xu, E., et al., 2019. Astragaloside IV ameliorates motor deficits and dopaminergic neuron degeneration via inhibiting neuroinflammation and oxidative stress in a Parkinson's disease mouse model. Int Immunopharmacol. 75, 105651.
Wang, L.Y., Yu, X., Li, X.X., et al., 2019a. Catalpol exerts a neuroprotective effect in the MPTP mouse model of Parkinson's disease. Front Aging Neurosci. 11, 316.
Kölliker-Frers, R., Udovin, L., Otero-Losada, M., et al., 2021. Neuroinflammation: an integrating overview of reactive-neuroimmune cell interactions in health and disease. Mediat. Inflamm., 9999146
Hinkle, J.T., Patel, J., Panicker, N., et al., 2022. STING mediates neurodegeneration and neuroinflammation in nigrostriatal α-synucleinopathy. Proc. Natl. Acad. Sci. (15), e2118819119
Zhang, C., Zhao, M., Wang, B., et al., 2021b. The Nrf2-NLRP3-caspase-1 axis mediates the neuroprotective effects of celastrol in Parkinson's disease. Redox Biol. 47, 102134.
Wang, Z., Zhang, S., Xiao, Y., et al., 2020. NLRP3 inflammasome and inflammatory diseases. Oxid. Med Cell Longev. 4063562.
Pike, A.F., Varanita, T., Herrebout, M.A.C., et al., 2021. α-Synuclein evokes NLRP3 inflammasome-mediated IL-1β secretion from primary human microglia. Glia 69 (6), 1413–1428.
Xian, H., Watari, K., Sanchez-Lopez, E., et al., 2022. Oxidized DNA fragments exit mitochondria via mPTP- and VDAC-dependent channels to activate NLRP3 inflammasome and interferon signaling. Immunity 55 (8), 1370–1385.e8.
Qiu, Y., Huang, Y., Chen, M., et al., 2022. Mitochondrial DNA in NLRP3 inflammasome activation. Int Immunopharmacol. 108, 108719. https://doi.org/10.1016/j.intimp.2022.108719. Epub 2022 Mar 26. PMID: 35349960.
Mills, E.L., Kelly, B., O'Neill, L.A.J., 2017. Mitochondria are the powerhouses of immunity. Nat. Immunol. 18 (5), 488–498.
Weiß, J., Heib, M., Korn, T., et al., 2023. Protease-independent control of parthanatos by HtrA2/Omi. Cell Mol. Life Sci. 80 (9), 258.
Wang, X., Becker, K., Levine, N., et al., 2019b. Pathogenic alpha-synuclein aggregates preferentially bind to mitochondria and affect cellular respiration. Acta Neuropathol. Commun. 7 (1), 41.
Tang, D., Kang, R., Berghe, T.V., et al., 2019. The molecular machinery of regulated cell death. Cell Res 29 (5), 347–364.
Kam, T.I., Mao, X., Park, H., et al., 2018. Poly(ADP-ribose) drives pathologic α-synuclein neurodegeneration in Parkinson's disease. Science 362 (6414), eaat8407.
Tan, Y., Xu, Y., Cheng, C., et al., 2020. LY354740 reduces extracellular glutamate concentration, inhibits phosphorylation of Fyn/NMDARs, and expression of PLK2/pS129 α-Synuclein in mice treated with acute or sub-acute MPTP. Front. Pharm. 11, 498997.
Xu S.Y., Bian R.L., Chen X. Methodology of pharmacological experiment. Beijing(PK): People's Medical Publishing House. 2002.
Zhang, Q.S., Heng, Y., Mou, Z., et al., 2017. Reassessment of subacute MPTP-treated mice as animal model of Parkinson's disease. Acta Pharm. Sin. 38 (10), 1317–1328.
Wu, S.H., Shi, Y.J., An, Y.F., et al., 2022. Neuroprotective effect of cinnamaldehyde in MPTP-induced mouse model of subacute Parkinson's disease. China J. Chin. Mater. Med 47 (23), 6485–6493.
Xiao, Y., Ren, Q., Wu, L., 2022. The pharmacokinetic property and pharmacological activity of acteoside: a review. Biomed. Pharm. 153, 113296.
Gao, H., Dou, L., Shan, L., et al., 2018. Proliferation and committed differentiation into dopamine neurons of neural stem cells induced by the active ingredients of radix astragali. NeuroReport 29 (7), 577–582.
Gao, M.R., Wang, M., Jia, Y.Y., et al., 2020. Echinacoside protects dopaminergic neurons by inhibiting NLRP3/Caspase-1/IL-1β signaling pathway in MPTP-induced Parkinson's disease model. Brain Res Bull. 164, 55–64.
Zhang, W., Zhang, F., Hu, Q., et al., 2021c. The emerging possibility of the use of geniposide in the treatment of cerebral diseases: a review. Chin. Med 16 (1), 86.
Pizarro-Galleguillos, B.M., Kunert, L., Brüggemann, N., et al., 2023. Neuroinflammation and mitochondrial dysfunction in Parkinson's disease: connecting neuroimaging with pathophysiology. Antioxid. (Basel) 12 (7), 1411.
Liu, L., Wang, J., Wang, H., 2020. Hydrogen sulfide alleviates oxidative stress injury and reduces apoptosis induced by MPP+ in Parkinson's disease cell model. Mol. Cell Biochem 472 (1-2), 231–240.
Zhu, S., Xu, N., Han, Y., et al., 2022. MTERF3 contributes to MPP+ -induced mitochondrial dysfunction in SH-SY5Y cells. Acta Biochim Biophys. Sin. (Shanghai) 54 (8), 1113–1121.
Jayanti, S., Moretti, R., Tiribelli, C., et al., 2022. Bilirubin prevents the TH+ dopaminergic neuron loss in a Parkinson's disease model by acting on TNF-α. Inter J. Mole Sci. 23 (22), 14276.
Guo, S., Wang, H., Yin, Y., 2022. Microglia polarization from M1 to M2 in neurodegenerative diseases. Front Aging Neurosci. 14, 815347.

Giovannoni, F., Quintana, F.J., 2020. The role of astrocytes in CNS inflammation. Trends Immunol. 41 (9), 805–819.
Zhang, Z., Venditti, R., Ran, L., et al., 2023. Distinct changes in endosomal composition promote NLRP3 inflammasome activation. Nat. Immunol. 24 (1), 30–41.
Calabresi, P., Mechelli, A., Natale, G., et al., 2023. Alpha-synuclein in Parkinson's disease and other synucleinopathies: from overt neurodegeneration back to early synaptic dysfunction. Cell Death Dis. 14 (3), 176.
Yao, M.F., Dang, T., Wang, H.J., et al., 2024. Mitochondrial homeostasis regulation: a promising therapeutic target for Parkinson's disease. Behav. Brain Res 459, 114811.
Giamogante, F., Barazzuol, L., Maiorca, F., et al., 2024. A SPLICS reporter reveals [Formula: see text]-synuclein regulation of lysosome-mitochondria contacts which affects TFEB nuclear translocation. Nat. Commun. 15 (1), 1516.
Huang, Q., Yang, P., Liu, Y., et al., 2023. The interplay between α-synuclein and NLRP3 inflammasome in Parkinson's disease. Biomed. Pharm. 168, 115735.